

1 Illumination stimulates cAMP receptor protein-dependent  
2 transcriptional activation from regulatory regions containing class I  
3 and class II promoter elements in *Synechocystis* sp. PCC 6803.

4  
5  
6  
7 Cell and Molecular Biology of Microbes

8  
9  
10  
11  
12  
13  
14  
15  
16 Jennifer Hedger<sup>1,3</sup>, Peter C. Holmquist<sup>1</sup>, Kimberly A. Leigh<sup>2</sup>, Kumuda Saraff<sup>1</sup>, Christina  
17 Pomykal<sup>1</sup>, and Michael L. Summers<sup>1\*</sup>

18  
19 <sup>1</sup>California State University Northridge, Department of Biology, 18111 Nordhoff St.  
20 Northridge, CA 91330

21 <sup>2</sup>Amgen, Thousand Oaks, CA 91320

22 <sup>3</sup>Present address: C3 Jian, Inc., Inglewood, CA 90301

23  
24 \*corresponding author. Tel.: +1-818-677-7146; fax.: +1-818-677-2034. E-mail address:  
25 [michael.l.summers@csun.edu](mailto:michael.l.summers@csun.edu)

26  
27 **Acronyms:**

28 cyclic adenosine monophosphate (cAMP), cAMP receptor protein (Crp or Sycrp1  
29 specifically in *Synechocystis*), wild-type (Wt), RNA polymerase (RNAP), intracellular  
30 cAMP ([cAMP]).

31  
32  
33  
34 **Keywords:**

35 cAMP, *crp*, *sycrp1*, promoter, gene expression.

37 **SUMMARY**

38

39 The cAMP receptor protein (Crp) is a global transcriptional regulator that binds  
40 sequence-specific promoter elements when associated with cAMP. In the motile  
41 cyanobacterium *Synechocystis* sp. strain PCC 6803, intracellular [cAMP] increases when  
42 dark-adapted cells are illuminated. Previous work has established that Crp binds  
43 proposed Crp target sites upstream of *slr1351* (*murF*), *sll1874* (*chlA<sub>II</sub>*), *sll1708* (*narL*),  
44 *slr0442*, and *sll1268* *in vitro*, and that *slr0442* is down-regulated in a *crp* mutant during  
45 photoautotrophic growth. To establish additional Crp target genes in *Synechocystis*,  
46 eleven different Crp binding sites proposed by a previous computational survey were  
47 tested for *in vitro* sequence-specific binding and *crp*-dependent transcription. The results  
48 indicate that *murF*, *chlA<sub>II</sub>*, and *slr0442* can be added as “target genes of Sycrp1” in  
49 *Synechocystis*. Promoter mapping of the targets revealed the same close association of  
50 RNA polymerase and Crp as that found in *Escherichia coli* class I and class II Crp-  
51 regulated promoters thereby strongly suggesting similar mechanisms of transcriptional  
52 activation.

53

54

55

56

57

58

59

60

61

## 62 INTRODUCTION

63  
64 The cyclic adenosine monophosphate (cAMP) receptor protein (Crp, or ‘Sycrp1’ in  
65 *Synechocystis* where required for clarity) can act as a transcriptional regulator when  
66 bound to the cAMP ligand (Botsford & Harman, 1992). Intracellular cAMP levels  
67 change dynamically to control gene regulation (Cann, 2004; Hammer *et al.*, 2006; Kolb  
68 *et al.*, 1993; Ohmori & Okamoto, 2004; Sakamoto *et al.*, 1991). Various environmental  
69 conditions signal *Synechocystis* to maintain low, moderate, and high [cAMP] levels that  
70 can be defined accordingly. Following dark adaptation, [cAMP] levels are low (0.02 to  
71 0.04 pmol cAMP ( $\mu\text{g Chl } a^{-1}$ ) (Terauchi & Ohmori, 2004). During regular  
72 photoautotrophic growth, [cAMP] levels are moderate (0.14 to 0.20 pmol cAMP ( $\mu\text{g Chl } a^{-1}$ )  
73 (Ochoa de Alda *et al.*, 2000; Terauchi & Ohmori, 1999). Following illumination  
74 with either blue or white light, dark-adapted cells increase [cAMP] to high levels (0.60 to  
75 0.80 pmol cAMP ( $\mu\text{g Chl } a^{-1}$ ) (Masuda & Ono, 2004; Terauchi & Ohmori, 1998;  
76 Terauchi & Ohmori, 2004). These spectrum-specific photoresponses support the current  
77 view that the cAMP/Crp complex may be ecologically beneficial for optimal positioning  
78 of motile cells relative to incident light (Bhaya *et al.*, 2006; Masuda & Ono, 2004).  
79 Indeed, it has been shown that intracellular cAMP ([cAMP]) is necessary and sufficient  
80 to restore phototactic motility used by cells to escape from the confines of a colony  
81 during suboptimal illumination (Bhaya *et al.*, 2006; Terauchi & Ohmori, 1999). Both  
82 Crp and cAMP are required for transcriptional activation of genes encoding type IV pilin  
83 biosynthesis proteins involved in motility thereby strongly suggesting a role for  
84 regulation of motility by Crp (Yoshimura *et al.*, 2002b; Yoshimura *et al.*, 2002a).

85  
86 To predict additional candidate genes for Crp regulation, a computational survey has  
87 previously proposed 11 different Crp binding target sequences based on the observation  
88 that Sycrp1 binds the *Escherichia coli* consensus ICAP Crp-binding site (Ochoa de Alda  
89 & Houmard, 2000). Recently, a biochemical study by Omagari *et al.* (2008)  
90 demonstrated *in vitro* that systematic substitution of bases in ICAP could be used to fairly  
91 accurately predict the observed free energy change ( $\Delta\Delta G_{\text{total}}^A$ ) of Crp binding to any  
92 given DNA sequence (Omagari *et al.*, 2008). The limit for detection of Crp binding *in*  
93 *vitro* was  $< 3.1 \Delta\Delta G_{\text{total}}^A$ , and all intergenic sequences in the *Synechocystis* genome  
94 containing calculated  $\Delta\Delta G_{\text{total}}^A < 3.1$  were bound by Crp. The study by Omagari *et al.*  
95 (2008) demonstrated Crp binding to three of the eleven target sequences (*slr1351*,  
96 *sll1874*, *sll1708*) predicted by Ochoa de Alda & Houmard (2000). Most recently, an  
97 interspecies bioinformatic comparison of cyanobacterial genomes (Xu & Su, 2009) has  
98 been performed based, in part, on probable Crp binding sites in the *Synechocystis* Crp  
99 transcriptome as identified by Yoshimura *et al.* (2002). Of the fifty-three target  
100 sequences Xu & Su (2009) predicted for *Synechocystis*, seven (*slr1732*, *slr1667*, *slr1351*,  
101 *sll1708*, *sll1874*, *slr0442*, *sll1268*) were bound by Crp in the Omagari *et al.* (2008) study,  
102 and three (*slr1351*, *sll1708*, *sll1874*) were also predicted by Ochoa de Alda & Houmard  
103 (2000). These predictive and *in vitro* binding studies have not provided *in-vivo* evidence,  
104 nor elucidated possible mechanisms of transcriptional activation by Crp (i.e.- do Sycrp1-  
105 dependent promoters demonstrate the same well characterized promoter organization as  
106 in *E. coli*).

107

108 In an attempt to elucidate possible mechanisms of transcriptional activation by Crp,  
109 sequence-specific Crp/DNA binding, transcriptional start sites, and Crp-dependent  
110 regulation of the *slr1667-1668* operon were demonstrated (Yoshimura *et al.*, 2002a).  
111 Even though the results did not establish a plausible mechanism (see discussion), this  
112 operon has subsequently been discussed in the context of Crp regulation (Dienst *et al.*,  
113 2008; Singh *et al.*, 2008; Summerfield & Sherman, 2008). Further, the Kazusa  
114 Cyanobase describes these genes as “target genes of Sycrp1” based on data that  
115 demonstrated both: 1) *in vitro* sequence-specific binding and 2) Crp-dependent gene  
116 expression. These two criteria will be referenced as such throughout this text. No other  
117 genes have been so annotated in the *Synechocystis* genome to date.

118  
119 To establish additional “target genes of Sycrp1”, all Crp targets proposed by Ochoa de  
120 Alda & Houmard (2000) and a target (*slr0442*) proposed by Omagari *et al.* (2008) were  
121 studied using a motile *Synechocystis* strain capable of large increases in [cAMP]  
122 following illumination. These proposed targets were tested *in vitro* for sequence-specific  
123 Crp/DNA binding, and expression was monitored in Wt and *crp* cells to assess Crp-  
124 dependent regulation during a dark to light environmental change that causes a low to  
125 high [cAMP] change. The results indicate that *slr1351* (*murF*), *sll1874* (*chlAII*) and  
126 *slr0442* can be added as “target genes of Sycrp1” in *Synechocystis*. Plausible Crp  
127 activation mechanisms of these cyanobacterial Crp targets are discussed based on  
128 transcriptional start sites mapped in *Synechocystis* and similar expression of promoter  
129 reporter constructs derived from these targets and expressed in *E. coli*.

130

## 131 METHODS

132

133 **Strains and growth conditions.** The wild-type (Wt) motile glucose-sensitive  
134 *Synechocystis* PCC sp. strain 6803 was obtained from the Pasteur Culture Collection. All  
135 *Synechocystis* cells were pre-grown for 11 d in BG-11 medium (Stanier *et al.*, 1971)  
136 containing 75.0 mM TES pH 7.75, 10.0 mM bicarbonate, and were supplemented with  
137 5.0 mM bicarbonate every 12 h in a manner that maintained logarithmic growth at pH  
138 7.75 in an inorganic carbon-replete condition. *Synechocystis* cells were grown at 30 °C  
139 and illuminated with 30.0  $\mu\text{mol photons m}^{-2} \text{s}^{-1}$  from cool white fluorescent lamps.  
140 Cultures in mid-log phase (0.6 OD<sub>730</sub>) were washed in fresh media and transferred to the  
141 dark 16 h prior to sampling. Samples for RNA extraction were rapidly chilled on ice  
142 water, pelleted in a prechilled rotor for 10 min at 4 000 g, and flash frozen immediately  
143 following sampling in the dark, 30, and 60 min following illumination. *E. coli* K12  
144 M182  $\Delta\text{lac}$  Wt (Casadaban *et al.*, 1980; Casadaban & Cohen, 1980) and *crp* mutant  
145 (Busby *et al.*, 1983) stock cultures were kindly provided by Stephen Busby (University of  
146 Birmingham) and were maintained in Luria-Bertani (LB) medium supplemented with  
147 30.0  $\mu\text{g streptomycin ml}^{-1}$  and 50.0  $\mu\text{g ampicillin ml}^{-1}$  respectively. *E. coli* clones  
148 containing reporter plasmids were grown in LB with or without 3% glucose in a roller  
149 drum at 37 °C for 48 h and assayed for green fluorescent protein (Gfp) signal as  
150 described below. All antibiotics were omitted from experimental cultures. *E. coli* DH5 $\alpha$   
151 MCR was used for plasmid amplification.

152

153 **Molecular biology techniques.** Plasmid purifications, isolation, PCR, ligation reactions,  
154 southern blotting, and transformations were performed according to standard protocols  
155 (Ausubel *et al.*, 2000) using commercial kits for DNA purification. *Synechocystis* sp.  
156 PCC 6803 genomic DNA was harvested as previously described (Summers *et al.*, 1995).

157  
158 ***sycr1* mutant construction.** The *sycr1* gene (*sll1371*) was amplified from genomic  
159 DNA using primers ATTCAGAGTTTACTGAGCGT and  
160 CCTGAGTTGGCCACACTGA and cloned into pCR2.1 (Invitrogen). The cloned gene  
161 was then inactivated by insertion of a *PvuII* fragment of pZeo (Stevens *et al.*, 1996),  
162 containing the *ble* zeocin resistance gene, into the *SmaI* site within *sll1371* to produce  
163 pKL2. This insertion was verified by sequencing at the California State University  
164 sequencing facility. The Wt strain was subject to natural transformation with pKL2 and  
165 selection in zeocin to yield cyclic adenosine monophosphate receptor protein *sycr1::ble*  
166 mutants (*crp*). Zeocin-resistant *crp* mutant stock cultures were maintained in BG-11  
167 supplemented with 6.0  $\mu\text{g zeocin ml}^{-1}$ .

168  
169 **Gfp reporter construction and quantification.** A novel *SphI* site was introduced into  
170 the multiple cloning site of the pIGA transcriptional reporter plasmid (Kunert *et al.*,  
171 2000) via a custom adaptor created by annealing  
172 GAGGGTACCGCATGCGGTACCTCA and TGAGGTACCGCATGCGGTACCCTC.  
173 *KpnI* digestion and ligation of the adapter (*KpnI-SphI-KpnI*) located downstream of a  
174 strong T7 transcription terminator sequence, but upstream of *gfp*, into the *KpnI* site of  
175 pIGA created pIGS. The promoter region and 5' amino terminus of the indicated  
176 *Synechocystis* genes were amplified by PCR using gene-specific primer sets  
177 (Supplementary Table 1) that added restriction sites for *KpnI* or *SphI*. The PCR product  
178 was digested, and ligated into pIGA or pIGS. Primers flanking the multiple cloning site  
179 (Argueta *et al.*, 2004) were used to sequence each insert thereby confirming the proper  
180 orientation and absence of mutation. The *slr0442* reporter construct was created by  
181 ligation of a partial *Hsp92II* *Synechocystis* genomic digest into pIGS and screening of *E.*  
182 *coli* DH5 $\alpha$  clones with and without glucose. The identified clone contained the almost  
183 complete *slr0442* intergenic region from chromosomal positions 2080200 to 2080940  
184 (Kaneko *et al.*, 1996). These resultant reporter plasmids were used to transform *E. coli*  
185 strains via electroporation followed by selection in LB supplemented with 50.0  $\mu\text{g}$   
186 kanamycin  $\text{ml}^{-1}$ .

187  
188 *E. coli* cells containing reporter constructs were washed twice in phosphate-buffered  
189 saline and normalized to 0.25 OD<sub>595</sub> immediately prior to measuring fluorescence as  
190 previously described (Argueta & Summers, 2005).

191  
192 **RNA isolation and reverse transcriptase-mediated quantitative PCR (RT-QPCR).**  
193 RNA was isolated as previously described (Byung-Hyuk Kim *et al.*, 2006) and visualized  
194 for integrity in a formaldehyde gel. Genomic DNA was removed by two rounds of RQ1  
195 DNase (Promega) digestion and Zymoclean (Zymo Research) column purification  
196 according to the manufacturer's instructions. The absence of genomic DNA in the  
197 resultant RNA samples was confirmed by the absence of product following PCR using  
198 *mnpB* primers and a genomic control. RNA samples were normalized to 1.0  $\text{g l}^{-1}$  and

199 frozen once at  $-80^{\circ}\text{C}$  prior to RT-QPCR. Reverse transcription was performed using  
200 reverse primers (Table S1) and SuperscriptII<sup>TM</sup> (Invitrogen) according to the  
201 manufacturer's instructions using 1.0  $\mu\text{g}$  RNA to generate cDNA. RT-QPCR was  
202 performed using 13.0  $\mu\text{l}$  of Power SYBR green PCR master mix (Applied Biosystems),  
203 2.0  $\mu\text{l}$  of cDNA serial dilutions and gene specific primer sets (Supplementary Table 1) at  
204 a final concentration of 300 nM primer each in a final volume of 26.0  $\mu\text{l}$ . Temperature  
205 cycles in an ABI 7300 Real-Time PCR were 10 min at  $95^{\circ}\text{C}$ , 35 cycles of 15 s at  $95^{\circ}\text{C}$ ,  
206 25 s at  $51^{\circ}\text{C}$ , and 1 min at  $72^{\circ}\text{C}$  followed by a slow melt cycle to confirm specific  
207 product formation. Gel electrophoresis was also performed to confirm absence of non-  
208 specific PCR products in experimental samples and controls. Six serial dilutions of each  
209 cDNA sample were used per target and reference sample, and the relative expression  
210 between Wt and *crp* transcripts was calculated as described (Pfaffl, 2001) using *mnpB* as  
211 an internal calibrator (Fernandez-Gonzalez *et al.*, 1998). All PCR efficiencies calculated  
212 by serial dilution were within 10% of expected doubling, and *mnpB* transcript levels  
213 yielded consistent PCR cycle fluorescence thresholds relative to total RNA for all  
214 samples.

215

216 **Rapid amplification of cDNA ends (RACE).** The +1 start site of transcription was  
217 determined for selected genes using nested intragenic primers (Table S1) and 1.0  $\mu\text{g}$  total  
218 RNA for RACE analysis as previously described (Argueta *et al.*, 2006).

219

220 **Protein purification and electromobility gel shift assay (EMSA).** Masayuki Ohmori  
221 (Saitama University) kindly provided pCGA used to overexpress histidine-tagged His-  
222 Sycrp1. A method for purification, binding reactions, and EMSA has been previously  
223 been described (Yoshimura *et al.*, 2000) and was essentially reproduced.

224

225 Following induction with IPTG, BL21(DE3) *E. coli* cells containing pCGA and pLysS  
226 were washed in lysis buffer. Lysis and purification was performed at  $4^{\circ}\text{C}$ . Cells were  
227 disrupted by sonication and the lysate was clarified by ultracentrifugation at 150 000 *g*  
228 for 45 min. Following loading and washing with four column volumes of lysis buffer,  
229 nickel and mono-Q columns were eluted using gradients to 400 mM imidazole (10 mM  
230 wash buffer) and 1.0 M NaCl respectively over 10 column volumes in 50 mM NaCl, 1.0  
231 mM  $\beta$ -mercaptoethanol, 50.0 mM Tris pH 8.0 and 10 % v/v glycerol. This solution was  
232 also used for between-column dialysis and as a lysis buffer. Homogeneity of the purified  
233 protein was confirmed by SDS-PAGE and Western blot detection using Tetra-His  
234 antibody. Binding activity specific to the purified protein was confirmed by visualization  
235 of the His-Sycrp1 in complex with *slr1667* and not in complex with Rndm. (see Table 1  
236 for substrate sequences) using native-PAGE (described below) and a Tetra-His antibody.  
237 The blocking reagent and Tetra-His antibody conjugated to horseradish peroxidase from  
238 Qiagen, and Supersignal CL-HRP visualization substrate from Novagen, were used  
239 according to manufacturer's recommendations.

240

241 5' phosphate-free oligonucleotides were synthesized by Integrated DNA Technologies  
242 without HPLC purification, mixed 1 to 1 with their complement, annealed by boiling  
243 followed by slow cooling over 3 h, and gel purified by UV shadowing following native-  
244 PAGE of DNA alone. This process allowed visualization of bands for excision and

245 overnight extraction in 10 mM Tris pH 8.0, which yielded pure 40' mer dsDNA for  
246 quantification. T4 polynucleotide kinase from Invitrogen was used as per manufacturer's  
247 instruction to label blunt-end double-stranded oligonucleotides indicated (Table 1) using  
248  $11\ 100 \times 10^{10}$  Bq (mmol [ $\gamma$ - $^{32}$ P]ATP) $^{-1}$ . Unincorporated label was removed with Bio-  
249 GelP-6 (#116561) from Bio-Rad as per manufacturer's instructions.

250  
251 For native-PAGE gel shift experiments, the binding reaction buffer contained 20  $\mu$ M  
252 cAMP, 1.0 nM labeled dsDNA, His-Sycrp1 as indicated, 50mM Tris-HCl pH 7.5, 60 mM  
253 NaCl, 1.0 mM EDTA, 8.3 % glycerol, and 0.1 mg/ml acetylated bovine serum albumin  
254 (BSA). Reactions were incubated at 22° C for 25 min, then on ice for 15 min. The  
255 reactions were quickly, and directly, loaded on the gel without loading buffer or dye. 90  
256 V was immediately applied for 10 min, and then increased to 200 V for an additional 35  
257 to 45 min. The gel apparatus and buffers were pre-chilled and maintained at 4 °C. 90 V  
258 was applied for at least 30 min prior to loading to remove mobile charged molecules. All  
259 running buffers were titrated to pH 8.0 to match the reaction buffer at 4 °C. All gels,  
260 running buffers, and reaction buffers contained 20  $\mu$ M cAMP (except where noted).  
261 Reagents were not filtered following addition of BSA or cAMP to maintain the indicated  
262 concentrations. The experiment specific tris acetate EDTA (TAE), tris borate EDTA  
263 (TBE), and components varied in the reaction buffer are indicated in Figure 1. Gels were  
264 visualized by exposure to x-ray film at -80° C.

265  
266 **Multiple Sequence Alignment (MSA).** MSA's were constructed using Clustal W in  
267 Biology Workbench (<http://workbench.sdsc.edu/>) (Subramaniam, 1998).

268

## 269 RESULTS

270

### 271 Crp sequence-specific binding was demonstrated

272

273 To demonstrate Crp binding *in vitro*, a positive binding control *slr1667*, a randomly  
274 generated sequence, and all target sites proposed by Ochoa de Alda & Houmard (2000)  
275 were screened for Crp binding (Fig. 1a, Table I). The *chlAII*, *narL*, and *murF* target sites  
276 were bound by His-Sycrp1. These proposed target sites are the only loci common to all  
277 Omagari *et al.* (2008), Ochoa de Alda & Houmard (2000), and Xu & Su (2009)  
278 predictions. These results were in accord with the inability of Omagari *et al.* (2008) to  
279 detect binding to any proposed site that has a calculated  $\Delta\Delta G_{total}^A > 3.1$ . In Figure 1(a),  
280 binding to *narL* was detected,  $\Delta\Delta G_{total}^A = 3.1$ ; consequently, sensitivity similar to that  
281 achieved by Omagari *et al.* (2008) was demonstrated in this assay. The  $K_d$  of His-SyCrp1  
282 from all proposed targets bound in Figure 1 has been described (Omagari *et al.*, 2008).  
283 In side-by-side experiments, all previously published interactions were detected and yet  
284 failed to identify any new interactions among targets proposed by Ochoa de Alda &  
285 Houmard (2000).

286

287 To demonstrate cAMP dependence for Crp/DNA binding in our *in vitro* binding  
288 conditions, all oligonucleotides listed in Table 1 were assayed exactly as in Fig. 1(a)  
289 except cAMP was omitted from the reaction, running buffers, and gels. Likely due to a  
290 combination of high affinity (even greater than that for the *E. coli* consensus ICAP)

291 (Omagari *et al.*, 2008) and cAMP carried over from *E. coli* expression, Crp binding to the  
292 proposed *murF* target was detectable. However, binding was severely reduced to < 10 %  
293 bound as opposed to 100 % in the presence of 20  $\mu$ M cAMP. Detectable binding was  
294 absent in all other instances (data not shown).

295  
296 To further demonstrate reproducibility and sequence-specificity for these proposed  
297 binding sites, competition assays were performed (Fig. 1b and c). The putative Crp  
298 binding sites located upstream of *slr0442* and *sll1268* were also included. Expression of  
299 *slr0442* was down-regulated in a *crp* mutant (Yoshimura *et al.*, 2002a); consequently,  
300 *slr0442* was used as a positive control. The *sll1268* target proposed by Omagari *et al.*  
301 (2008) was included because of the high degree of conservation between it and *slr0442* in  
302 the intergenic and N-terminal coding regions. Our results demonstrated His-Sycrpl  
303 sequence-specific binding to *murF*, *narL*, *chlA<sub>II</sub>*, *slr0442*, and *sll1268* proposed targets  
304 via competition assays using the *slr1667* target as a specific competitor (Yoshimura *et al.*,  
305 2002a) and a random 40-mer (Rndm.) as a non-specific competitor. In all cases, the  
306 unlabeled specific competitor titrated Crp away from the labeled complex in favor of the  
307 specific competitor, while unlabeled non-specific competitor did not. Crp does not bind  
308 the *slr1667* target in the absence of cAMP *in vitro* as reported (Yoshimura *et al.*, 2002a),  
309 and reproduced here (see above). Consequently, titration by competitors further  
310 demonstrated the presence of Crp/cAMP complex. Omagari *et al.* (2008) has previously  
311 established the Crp sequence specificity to these proposed targets by correlation. Shown  
312 in Figure 1(b) and (c) is the first verification of specificity by direct competition. These  
313 results confirmed that the *murF*, *narL*, *chlA<sub>II</sub>*, *slr0442*, and *sll1268* intergenic sites  
314 described in Table 1 met sequence-specific binding criteria.

315  
316 Owing to complex instability during electrophoresis at room temperature as evidenced by  
317 smearing between bands in the work of Omagari *et al.* (2008) and reproduced in this  
318 work (data not shown), electrophoresis at 4 °C was performed. Despite the strong signal  
319 from labeled DNA, increased complex stability at 4 °C was demonstrated because  
320 smearing between bands was minimal to absent. However, at 4 °C, Crp/DNA complexes  
321 precipitated in 0.25  $\times$  TBE, which rendered them immobile by electrophoresis. Addition  
322 of 500 nM Rndm. completely restored solubility and allowed near 100 % binding as  
323 shown by *slr1667* and *murF* targets (Fig. 1a). As little as 0.5 mg l<sup>-1</sup> double-stranded poly  
324 deoxyinosinic-deoxycytidylic acid (poly-dIdC) added to the reaction buffer also restored  
325 solubility but reduced the fraction of Crp/DNA complex by 60 % (data not shown).  
326 Crp/DNA complexes were soluble in 1.0  $\times$  TAE at 4 °C, but low Crp affinity targets  
327 ( $\Delta\Delta G^A_{\text{total}} > 0.7$ ) did not maintain Crp/DNA complexes in this running buffer.  
328 Consequently, electrophoresis of *narL* and *chlA<sub>II</sub>* was performed in 0.25  $\times$  TBE. From  
329 these results, it is clear that temperature and ionic strength of electrophoresis buffers  
330 greatly affect Crp/DNA complex detection by gel shift.

331  
332 **The *sycrpl* mutant construction was gene specific, and did not introduce polar**  
333 **effects**

334  
335 To allow examination of Crp-dependent functions, a *crp* mutant was constructed by  
336 insertional inactivation of *sycrpl*. Complete segregation was confirmed by PCR.



337 Southern blotting further confirmed recombination had occurred specifically in the  
338 *sycrp1* locus and that *sll1924* (*sycrp2*) or *slr0593* homologues were not disrupted (data  
339 not shown). Additional evidence for gene inactivation was obtained by observing  
340 phototactic and *crp* non-motile phenotypes (Yoshimura *et al.*, 2002b) (data not shown).  
341 To discount polar effects of genes surrounding the site of *sycrp1* inactivation, transcript  
342 abundance of the two genes flanking *sycrp1* (*sll1370* and *sll1372*) was quantified in  
343 photoautotrophically growing cultures by RT Q-PCR. The quantities of these transcripts  
344 in the Wt did not differ detectably from those in *crp* mutant strains (Vasquez,  
345 unpublished). To determine whether Crp function was absent in the *crp* mutant, Wt and  
346 *crp* crude cell extracts were also assayed for binding to the *slr1667* target. Sequence-  
347 specific binding was absent in the *crp* mutant crude extracts but present in Wt samples  
348 (data not shown). Therefore, gene expression differences were ascribed specifically to  
349 inactivation of the *sycrp1* locus and resultant protein inactivation rather than to polar  
350 effects or recombination at non-target sites.

351

### 352 **The shift from dark to light environmental conditions stimulated Crp-dependent** 353 **transcriptional activation**

354

355 To confirm that [cAMP] increased under the experimental conditions described, [cAMP]  
356 was quantified by a cell filtration method. Intracellular cAMP increased from 0.046 to  
357 0.92 pmol cAMP ( $\mu\text{g Chl } a$ )<sup>-1</sup> following a dark (low [cAMP]) to light (high [cAMP])  
358 transition. These values were in good agreement with those previously reported (see  
359 introduction).

360

361 To quantify transcript levels, RNA samples were collected in the dark and at 30 and 60  
362 min after illumination. Cultures were sampled over one hour because transcriptional  
363 profiles are most dynamic during this period (Gill *et al.*, 2002). All target transcripts  
364 proposed by Ochoa de Alda & Houmard (2000) were quantified in a low-resolution  
365 screen. RNA was sampled from one culture of Wt and one culture of *crp* cells ( $n = 1$ ) to  
366 focus effort on demonstrating the reproducibility of Crp-dependent transcription reported  
367 below. Primer pair amplification efficiencies were not considered in this low-resolution  
368 screen comparing relative expression; consequently, we employed a prudent two-fold  
369 expression cut-off to differentiate between candidate Crp-dependent and Crp-independent  
370 expression. The *slr0194* (*rpiA*) transcript was one of nine proposed targets that did not  
371 demonstrate Crp-dependent transcription in this low-resolution screen. Consequently, it  
372 was used as a negative, Crp-independent, transcription control. Only *murF* and *chlA<sub>II</sub>*  
373 demonstrated more than two-fold Crp-dependent expression out of the eleven targets  
374 proposed by Ochoa de Alda & Houmard (2000) tested in this low-resolution screen.

375

376 Transcription of *rpiA*, *murF*, *chlA<sub>II</sub>*, and *slr0442* were further characterized to determine  
377 Crp-dependence following dark to light environmental changes (Fig. 2). Wt and *crp* cells  
378 were again cultured, this time in triplicate ( $n = 3$ ) to demonstrate reproducibility, and  
379 transcripts were quantified by RT-QPCR more accurately taking amplification efficiency  
380 into account. The positive transcription control *slr0442* was not activated in the Wt  
381 either 30 min (grey bars) or 60 min (white bars) following illumination (Fig. 2a). The  
382 quantity of detectable transcript was constant for all time points versus the initial low

383 [cAMP] condition and resulted in an expression ratio of 1.0. Conversely, transcript levels  
384 in the mutant decreased following illumination (Fig. 2b). After one hour of illumination,  
385 Wt expression of *slr0442* was five times greater than that of the mutant (Fig. 2c) and  
386 almost twice that reported during moderate [cAMP] growth conditions (Yoshimura *et al.*,  
387 2002a). Consequently, it was inferred that the constant *slr0442* expression in Wt cells  
388 was due to a steady state achieved by simultaneous transcriptional activation by Crp and  
389 posttranscriptional mRNA degradation.

390

391 This inference is supported by evidence that both *crp* and *ssr3321* (*hfq* candidate) single  
392 mutants display striking similarity in expression of *slr2015-2018*, *slr1667-1668*, and  
393 *slr0442*, which are down-regulated approximately 4-5, 40-48, and 3 fold respectively  
394 relative to Wt cells during regular photoautotrophic growth (Dienst *et al.*, 2008;  
395 Yoshimura *et al.*, 2002a). Hfq is a RNA-binding protein that acts to stabilize transcripts  
396 as a RNA chaperone or to facilitate the coupled degradation of sRNA-mRNA-duplexes  
397 (Dienst *et al.*, 2008). Although the mechanism of Hfq activity has not yet been  
398 demonstrated in cyanobacteria, it could explain posttranscriptional modification of  
399 *slr1667* and *slr0442*. Under high-light stress, the 3' mRNA of *slr1667* is sixty-fold more  
400 abundant than the 5'-end (Singh *et al.*, 2008). This finding clearly demonstrates strong  
401 post-transcriptional mRNA degradation that could plausibly be stabilized by a functional  
402 RNA chaperone.

403

404 Assessment of *slr0442* expression yielded similar results, suggesting that the 5' mRNA  
405 was unstable. For example, RT-QPCR results were not reproducible using either of two  
406 different primer sets targeted to the 5' mRNA of *slr0442*, even though accurate  
407 quantification of a genomic DNA control using the same primers was possible (data not  
408 shown). However, amplification of the 3' end yielded clear results as shown (Fig. 2). All  
409 other transcripts in this work were successfully amplified from their 5' ends. Difficulties  
410 attaining consistent RT-QPCR results for the 5' end of *slr0442* transcript and the  
411 decreasing expression during illumination of *crp* cells were consistent with  
412 posttranscriptional mRNA degradation following illumination in the absence of Crp.

413

414 Wt and mutant transcript levels for all genes in Fig. 2 were approximately equal in dark-  
415 adapted cells when [cAMP] is low. Transcripts of *murF* and *chlA<sub>II</sub>* were up-regulated by  
416 illumination but showed four and ten times respectively more transcript expression  
417 relative to the mutant following [cAMP] increase, thus demonstrating strong Crp  
418 dependence for transcription activation. In contrast, transcription from the negative  
419 transcription control *rpiA* did not exhibit Crp dependence even though it was strongly  
420 induced following illumination (Fig. 2a and b). In sum, these results demonstrated that  
421 transcription from *murF*, and *chlA<sub>II</sub>*, and *slr0442* met Crp-dependent expression criteria.

422

### 423 **Expression driven by Sycrp1 “target” promoters required Crp in *E. coli***

424

425 To determine if the transcriptional machinery in *E. coli* was sufficient to stimulate Crp-  
426 dependent transcription from Crp “target” promoters, all target promoters proposed by  
427 Ochoa de Alda & Houmard (2000) were oriented to drive transcription of a *gfp* reporter  
428 in Wt and *crp* mutant strains of *E. coli*. Transcripts from cells grown in the high [cAMP]

429 condition demonstrated Crp-dependent activation. The glucose effect is well documented  
430 (Kolb *et al.*, 1993) and causes a drastic drop in [cAMP]. To decrease [cAMP], glucose  
431 was added to the culture.

432

433 The positive transcription control *slr0442* was strongly induced in the Wt during high  
434 [cAMP] growth without glucose (Fig. 2d), but not in the mutant (Fig. 2e). Although Wt  
435 expression was four times that of the mutant during the low [cAMP] growth condition  
436 with glucose (Fig. 2f), expression was 60 times greater in the high [cAMP] condition  
437 thereby demonstrating a strong Crp activation dependence. Although not shown, it is  
438 interesting to note that the Wt strain repressed *narL* transcription in the high [cAMP]  
439 condition 10 times more than in the *crp* mutant. The *narL* reporter was also  
440 independently isolated from the *Hsp92II* genomic reporter library due to similar  
441 expression characteristics (data not shown). Otherwise, in general, the *E. coli* reporter  
442 data paralleled results seen in *Synechocystis* excepting *chlA<sub>II</sub>*. In this case, absolute  
443 fluorescence was indistinguishable from background fluorescence, indicating that the  
444 *chlA<sub>II</sub>* promoter did not drive transcription in *E. coli*. The background fluorescence  
445 between *E. coli* M182 Wt and *crp* strains containing the *gfp* reporter plasmid but lacking  
446 the indicated intergenic regions were indistinguishable (data not shown). All other  
447 indicated constructs yielded signals well above this background. Consequently, these  
448 data demonstrated that the transcriptional elements in *E. coli* were sufficient to stimulate  
449 Crp-dependent transcription from *slr0442*, and *murF* intergenic regions.

450

#### 451 **Transcription start sites were determined**

452

453 All presented transcription +1 start sites for *murF*, *narL*, *chlA<sub>II</sub>*, *slr0442*, and *sll1268* were  
454 determined by RACE in this work (Fig. 3). These promoters are accordingly labeled in  
455 Figure 3, and the most distal from the gene is assigned P<sub>1</sub>. We are unaware of any other  
456 studies mapping start sites for these genes. It should be noted that RACE requires much  
457 less transcript than primer extension due to its high sensitivity. However, RACE is not a  
458 quantitative method; consequently, the relative strengths of these promoters as affected  
459 by Crp activation were not inferred.

460

461 RNA from both Wt and *crp* strains experiencing both low and high [cAMP] all yielded  
462 the same start sites although  $\pm 1$  base chatter between samples was observed at *murF* P<sub>2</sub>  
463 (Fig. 3a). P<sub>1</sub> TGGTAAGATACACCCTG (transcriptional start site in italicized bold) is  
464 not shown and lies 136 bases upstream of P<sub>2</sub>. *Crocospaera watsonii* and *Cyanothece* sp.  
465 CCY 0110 MurF whole protein BLAST scores were 9e-136 and 1e-129, respectively,  
466 relative to *Synechocystis* MurF. The intergenic and non-conserved N-terminal *murF*  
467 regions from these closely related cyanobacteria were aligned to highlight other  
468 conserved elements because of an apparent conservation of the proposed Crp site. A total  
469 of 30 and 31 base gaps were observed for *Crocospaera* and *Cyanothece* respectively in  
470 the region between the conserved Crp core binding sequence and strongly conserved  
471 protein coding region. These deletions corresponded almost exactly to three 10.5-bp  
472 turns of the alpha helix. In the alignments shown, a 12-bp gap that corresponds to  
473 approximately one helical turn is located between P<sub>3</sub> and the putative Crp binding site.

474

475 The intergenic *chlA<sub>II</sub>* region contained only one putative transcriptional start site (Fig.  
476 3b). Similar sequence alignments of intergenic regions from *chlA* orthologues of these  
477 closely related cyanobacteria were uninformative due to low sequence homology and  
478 absence of readily identifiable Crp site core sequences. Consequently, an alignment is  
479 not shown.

480

481 The *slr0442* and *sll1268* intergenic sequences were aligned because the encoded proteins  
482 of these genes bear 75% identity within the first 58 amino terminal amino acids and the  
483 proposed Crp sites were roughly equidistant from the common, not the annotated, ATG  
484 start codon (Fig. 3c). Only one base spacing difference was observed between  
485 transcription start and proposed Crp sites for these two gene promoters.

486

## 487 **DISCUSSION**

488

### 489 **Some proposed “Target genes of Sycrp1” may not have been detected**

490

491 The utility of dark to light conditions for elucidating Crp-dependent activation as  
492 proposed by Omagari *et al.* (2008) has been demonstrated by the results reported here.  
493 Predicted targets were up-regulated in a Crp-dependent manner only when predictions  
494 made by Ochoa de Alda & Houmard (2000), Xu & Su (2009), and Omagari *et al.* (2008)  
495 overlapped (Bold and underlined in Table 1). In all cases, excluding *narL*, those  
496 intergenic regions containing Crp core binding sites  $< 3.1 \Delta\Delta G^{\text{A}}_{\text{total}}$  were bound by His-  
497 Sycrp1 *in vitro* and demonstrated Crp-dependent activation *in vivo*. Consequently, *murF*,  
498 *chlA<sub>II</sub>*, and *slr0442* meet the “Target gene of Sycrp1” criteria used to annotate the Kazusa  
499 Cyanobase.

500

501 It is, however, conceivable that the low-resolution expression screen overlooked subtle  
502 expression differences such as those of the divergently transcribed regulatory genes *narL*  
503 and *slr1805* (*hik16* subunit). The possible protein-protein interactions suggested by yeast  
504 two-hybrid experiments where NarL interacted with Hik16 and MurC (Sato *et al.*, 2007)  
505 suggests protein level regulation in the first step of the peptidoglycan biosynthetic  
506 pathway three enzymatic reactions upstream of MurF-catalyzed ligation. Such regulation  
507 is expected to be involved in modulating the balance of intracellular carbon and nitrogen  
508 (Singh *et al.*, 2008).

509

510 Consistent with the only microarray data, to our knowledge, published using the motile  
511 glucose sensitive *Synechocystis* exposed to similar environmental conditions (Gill *et al.*,  
512 2002), the target transcripts in Fig. 2 that were proposed by Ochoa de Alda & Houmard  
513 (2000) were strongly up-regulated following illumination. Such up-regulation is also  
514 consistent with these gene products’ functions. Specifically, *murF* up-regulation is  
515 expected because its protein product is essential for peptidoglycan synthesis required for  
516 cell division during periods of growth (Malakhov *et al.*, 1995). Also, *chlA<sub>II</sub>* up-regulation  
517 upon illumination is expected because cultures that are dark adapted for prolonged  
518 periods and obtain oxygen equilibrium with the air are micro-oxic relative to actively  
519 photosynthesizing cultures. This micro-oxic state is achieved via the same mechanisms  
520 that cause diurnal dissolved oxygen cycles observed in lakes and cyanobacterial mats

521 (Jorgensen *et al.*, 1979). During micro-oxic illuminated conditions, *chlA<sub>II</sub>* is transcribed  
522 in a putative operon containing *ho2* (Sugishima *et al.*, 2005; Xu & Su, 2009; Zhang *et al.*,  
523 2005) and *hemN1* which catalyze three steps in the chlorophyll biosynthetic pathway  
524 (Minamizaki *et al.*, 2008). The Crp-dependent *chlA<sub>II</sub>* activation observed may suggest  
525 coordination between motility and photosynthetic acclimation, but requires further  
526 characterization of both pilin and *chlA<sub>II</sub>* Crp-dependent expression at these promoters.  
527

### 528 **Analysis of elements in Sycrp1 class I and II promoters**

529

530 Although mutagenesis was not used to demonstrate that the proposed Crp binding sites in  
531 Fig. 3 are required for gene activation, *in vivo* evidence exists to support such a  
532 conclusion. First, the conserved spacing of proposed Crp binding and +1 transcriptional  
533 start sites between these promoters and extensively characterized promoters of *E. coli*  
534 was observed. Second, *in vivo* transcriptional activation under conditions stimulating  
535 high [cAMP] required Crp in both *E. coli* and *Synechocystis*, thus demonstrating that  
536 transcription elements in *E. coli* are sufficient to stimulate Crp-dependent transcription  
537 from *murF* and *slr0442* intergenic regions (Fig. 2). Together these data indicate that the  
538 *E. coli* Crp mechanisms can be compared to those in *Synechocystis*.  
539

540 *E. coli* Crp promoters are classic model systems that have been thoroughly reviewed  
541 recently (Borukhov & Lee, 2005) and in the past (Busby & Ebright, 1999). By  
542 definition, Crp and RNA polymerase (RNAP) must be on the same side of the DNA  
543 strand to make contacts that stimulate transcription via the readily describable  
544 mechanisms of class I, class II, and class III promoters. Consequently, intervals of 10.5  
545 bp alpha-helical turns must be maintained from the middle of the -10 sigma factor  
546 binding site to the middle of the Crp site for Crp to contact RNAP. Five or more turns is  
547 defined as class I, and three turns a class II. Four-turn spacing does not occur because  
548 several Crp/RNAP interactions would be impeded. In *Synechocystis*, transcription start  
549 site mapping of the *slr1667-1668* operon revealed that the proposed Crp binding site is  
550 15.5 helical turns upstream from the middle of the -10 region thereby placing Crp on the  
551 opposite side of the DNA strand relative to RNAP (Yoshimura *et al.*, 2002a). In this  
552 case, Crp can not contact RNAP via the readily describable mechanisms outlined here.  
553 Consequently, the Crp activation mechanism at this locus is unclear. As opposed to class  
554 I and class II promoters, class III promoters require two or more activator molecules and  
555 RNAP for full transcription activation. A major difference between *E. coli* and  
556 cyanobacterial promoters is the frequent absence of a -35 sigma factor binding site  
557 (Curtis & Martin, 1994); however, the -10 region TATAAT is conserved and TANNNT  
558 is most frequently observed (Su *et al.*, 2005; Vogel *et al.*, 2003). The proposed class I  
559 and class II promoters described below are inferred based on this spacing until the  
560 involvement of an additional element is demonstrated to define class III organization.  
561

### 562 **The *murF* P<sub>3</sub> contains class I promoter spacing relative to the transcriptional start** 563 **site**

564

565 The *murF* P<sub>3</sub> bears class I promoter structure only in that the proposed Crp binding site is  
566 7.0 alpha helical turns from the transcriptional start site (Fig. 3a). However, the -10

567 region is not readily discernible within 4-7 bases of the transcriptional start. The only  
568 conserved TNNNNT sequence places Crp centered 5.7 helical turns away in suboptimal  
569 positioning but close to the same side of the DNA strand as the proposed sigma factor  
570 binding site. However, the spacing of these elements is not conserved among these  
571 freshwater cyanobacteria. Instead, deletions totaling three helical turns seem to have  
572 occurred independently because the deletions are not identical lengths. One is 30, the  
573 other 31 bp long. This keeps the elements that are retained on either side of the deletions  
574 in similar helical orientation and on same side of the DNA strand in the *Crocospaera*  
575 and *Cyanothece* sequences shown. Therefore, the observed conservation of helical  
576 spacing may be significant to regulation. Xu & Su (2009) predicted a -10 region,  
577 TAACAT, located 32 bp downstream from the proposed Crp binding site. This -10  
578 region is not properly positioned to initiate transcription from any of the +1 sites  
579 identified by RACE. Retention of the proposed Crp core binding sequences in these  
580 closely related cyanobacteria suggests that Crp regulation of *murF* is also conserved.

581

#### 582 **The *chlA<sub>II</sub>* promoter class is unclear**

583

584 The *chlA<sub>II</sub>* promoter class is unclear because the proposed Crp site is very distant and on  
585 the opposite face of the DNA strand relative to the transcriptional start site (Fig. 3b). The  
586 proposed Crp site is 28.6 helical turns from the transcriptional start site. Further, a  
587 plausible -10 region is not apparent; thus, we can not support the validity of this  
588 proposed transcriptional start site by relation to other conserved elements. Xu & Su  
589 (2009) predicted that a -10 region, TCGATT, is 29 bp downstream of the proposed Crp  
590 site; however, no +1 sites were identified by RACE in this region.

591

#### 592 **The *slr0442* P<sub>2</sub> contains class II promoter spacing**

593

594 The *slr0442* P<sub>2</sub> bears class II promoter structure maintaining the characteristic 3 alpha  
595 helical turn spacing between the center of the near consensus P<sub>2</sub> -10 region TAAAAT  
596 and the proposed Crp site (Fig. 3c). Crp binding would repress transcription from P<sub>1</sub> via  
597 steric hindrance of RNAP thereby switching most initiation to P<sub>2</sub>. The proposed intimate  
598 proximity with RNAP strongly suggests interactions between Crp and RNAP; however,  
599 analysis of activating regions 2 and 3 previously described in *E. coli* (see reviews cited  
600 above) by primary sequence alignment is insufficient to address the possibility of these  
601 interactions. The perfect alignment of the proposed Crp and -10 sites in both *slr0442* and  
602 *sll1268* was also predicted by Xu & Su (2009) and strongly suggests conservation of  
603 function as class II Crp promoter regulation. A second Crp site that was proposed by  
604 Omagari *et al.* (2008) (boxed with dashes in Fig. 3c), has not been confirmed by binding  
605 studies. It is optimally positioned on the same side as RNAP, thereby potentially  
606 implicating class III promoter structure.

607

608 The genes *slr0442* and *sll1268* are homologous within the amino terminal domain. This  
609 homology defines a large set of hitherto uncharacterized cyanobacterial proteins. The  
610 significance of this conserved region may suggest coordinated regulation of *slr0442* and  
611 *sll1268* by Crp.

612

613 As has been discussed above for *murF* and *slr0442*, promoter mapping revealed the same  
614 well characterized class I and class II promoter organization in *Synechocystis* as in *E.*  
615 *coli*. When intergenic regions containing these promoters were oriented to drive *gfp*  
616 transcription in *E. coli*, the results were parallel to the regulatory effects observed in  
617 *Synechocystis*. These results thereby illustrate structure and function associations *in vivo*  
618 (Fig. 2) and strongly suggest that cyanobacterial Crp-dependent promoter mechanisms  
619 can function similarly as in *E. coli*. Further, we provide the first experimental evidence  
620 to support the validity of forming bioinformatic predictions based on class II spacing of –  
621 10 and Crp site elements in cyanobacteria (Xu & Su, 2009).  
622

## 623 **Acknowledgements**

624  
625 The authors thank those who provided materials listed in the text, Cindy Malone for  
626 critical reading of the manuscript, and students who participated in the introductory  
627 molecular microbiology course and constructed reporter plasmids. This study was  
628 supported by grants from the NSF MCB 0099327, NIH 2 SO6 GM048680, to M.L.S. and  
629 a University Corporation project award for academic research, California State  
630 University, Northridge to J.H.

631  
632

## Reference List

- Argueta, C. & Summers, M. L. (2005).** Characterization of a model system for the study of *Nostoc punctiforme* akinetes. *Arch Microbiol* **183**, 338-346.
- Argueta, C., Yuksek, K., Patel, R. & Summers, M. L. (2006).** Identification of *Nostoc punctiforme* akinete-expressed genes using differential display. *Mol Microbiol* **61**, 748-757.
- Argueta, C., Yuksek, K. & Summers, M. (2004).** Construction and use of GFP reporter vectors for analysis of cell-type-specific gene expression in *Nostoc punctiforme*. *J Microbiol Methods* **59**, 181-188.
- Ausubel, F., Brent, R., Kingston, R., Moore, D., Seidman, J., Smith, J. & Struhl, K. (2000).** Current Protocols in Molecular Biology. U.S.A.: John Wiley & Sons, Inc.
- Bhaya, D., Nakasugi, K., Fazeli, F. & Burriesci, M. S. (2006).** Phototaxis and impaired motility in adenyl cyclase and cyclase receptor protein mutants of *Synechocystis* sp. Strain PCC 6803. *J Bacteriol* **188**, 7306-7310.
- Borukhov, S. & Lee, J. (2005).** RNA polymerase structure and function at *lac* operon. *C R Biol* **328**, 576-587.
- Botsford, J. L. & Harman, J. G. (1992).** Cyclic AMP in prokaryotes. *Microbiol Rev* **56**, 100-122.
- Busby, S., Kotlarz, D. & Buc, H. (1983).** Deletion mutagenesis of the *Escherichia coli* galactose operon promoter region. *J Mol Biol* **167**, 259-274.
- Busby, S. J. & Ebright, R. H. (1999).** Transcription activation by catabolite activator protein (CAP). *J Mol Biol* **293**, 199-213.
- Byung-Hyuk Kim, Hee-Mock Oh, Young-Ki Lee, Gang-Guk Choi, Chi-Yong Ahn, Byung-Dae Yoon & Hee-Sik Kim (2006).** Simple method for RNA preparation from cyanobacteria. *J Phycol* **42**, 1137-1141.
- Cann, M. J. (2004).** Signaling through cyclic nucleotide monophosphates in cyanobacteria. *New Phytol* **161**, 23-34.
- Casadaban, M. J., Chou, J. & Cohen, S. N. (1980).** In vitro gene fusions that join an enzymatically active beta-galactosidase segment to amino-terminal fragments of exogenous proteins: *Escherichia coli* plasmid vectors for the detection and cloning of translational initiation signals. *J Bacteriol* **143**, 971-980.
- Casadaban, M. J. & Cohen, S. N. (1980).** Analysis of gene control signals by DNA fusion and cloning in *Escherichia coli*. *J Mol Biol* **138**, 179-207.



- Curtis, S. E. & Martin, J. A. (1994).** The transcription apparatus and the regulation of transcription initiation. In *The Molecular Biology of Cyanobacteria*, pp. 613-639. Edited by D. A. Bryant. Norwell, MA, USA: Kluwer Academic Publishers.
- Dienst, D., Duhring, U., Mollenkopf, H. J., Vogel, J., Golecki, J., Hess, W. R. & Wilde, A. (2008).** The cyanobacterial homologue of the RNA chaperone Hfq is essential for motility of *Synechocystis* sp. PCC 6803. *Microbiol* **154**, 3134-3143.
- Fernandez-Gonzalez, B., Martinez-Ferez, I. M. & Vioque, A. (1998).** Characterization of two carotenoid gene promoters in the cyanobacterium *Synechocystis* sp. PCC 6803. *Biochim Biophys Acta* **1443**, 343-351.
- Gill, R. T., Katsoulakis, E., Schmitt, W., Taroncher-Oldenburg, G., Misra, J. & Stephanopoulos, G. (2002).** Genome-wide dynamic transcriptional profiling of the light-to-dark transition in *Synechocystis* sp. strain PCC 6803. *J Bacteriol* **184**, 3671-3681.
- Hammer, A., Hodgson, D. R. & Cann, M. J. (2006).** Regulation of prokaryotic adenylyl cyclases by CO<sub>2</sub>. *Biochem J* **396**, 215-218.
- Jorgensen, B. B., Revsbech, N. P., Blackburn, T. H. & Cohen, Y. (1979).** Diurnal cycle of oxygen and sulfide microgradients and microbial photosynthesis in a cyanobacterial mat sediment. *Appl Environ Microbiol* **38**, 46-58.
- Kaneko, T., Sato, S., Kotani, H., Tanaka, A., Asamizu, E., Nakamura, Y., Miyajima, N., Hirosawa, M., Sugiura, M., Sasamoto, S., Kimura, T., Hosouchi, T., Matsuno, A., Muraki, A., Nakazaki, N., Naruo, K., Okumura, S., Shimpo, S., Takeuchi, C., Wada, T., Watanabe, A., Yamada, M., Yasuda, M. & Tabata, S. (1996).** Sequence analysis of the genome of the unicellular cyanobacterium *Synechocystis* sp. strain PCC6803. II. Sequence determination of the entire genome and assignment of potential protein-coding regions. *DNA Res* **3**, 109-136.
- Kolb, A., Busby, S. J., Buc, H., Garges, S. & Adhya, S. (1993).** Transcriptional regulation by cAMP and its receptor protein. *Annu Rev Biochem* **62**, 749-795.
- Kunert, A., Hagemann, M. & Erdmann, N. (2000).** Construction of promoter probe vectors for *Synechocystis* sp. PCC 6803 using the light-emitting reporter systems Gfp and LuxAB. *J Microbiol Methods* **41**, 185-194.
- Malakhov, M. P., Los, D. A., Wada, H., Semenenko, V. E. & Murata, N. (1995).** Characterization of the *murF* gene of the cyanobacterium *Synechocystis* sp. PCC 6803. *Microbiol* **141**, 163-169.
- Masuda, S. & Ono, T. A. (2004).** Biochemical characterization of the major adenylyl cyclase, Cya1, in the cyanobacterium *Synechocystis* sp. PCC 6803. *FEBS Lett* **577**, 255-258.
- Minamizaki, K., Mizoguchi, T., Goto, T., Tamiaki, H. & Fujita, Y. (2008).** Identification of two homologous genes, *chlAI* and *chlAII*, that are differentially involved

in isocyclic ring formation of chlorophyll *a* in the cyanobacterium *Synechocystis* sp. PCC 6803. *J Biol Chem* **283**, 2684-2692.

**Ochoa de Alda, J. A., Ajlani, G. & Houmard, J. (2000).** *Synechocystis* strain PCC 6803 *cya2*, a prokaryotic gene that encodes a guanylyl cyclase. *J Bacteriol* **182**, 3839-3842.

**Ochoa de Alda, J. A. & Houmard, J. (2000).** Genomic survey of cAMP and cGMP signalling components in the cyanobacterium *Synechocystis* PCC 6803. *Microbiol* **146**, 3183-3194.

**Ohmori, M. & Okamoto, S. (2004).** Photoresponsive cAMP signal transduction in cyanobacteria. *Photochem Photobiol Sci* **3**, 503-511.

**Omagari, K., Yoshimura, H., Suzuki, T., Takano, M., Ohmori, M. & Sarai, A. (2008).** DeltaG-based prediction and experimental confirmation of SYCRP1-binding sites on the *Synechocystis* genome. *FEBS J.* **10**, 23-39

**Pfaffl, M. W. (2001).** A new mathematical model for relative quantification in real-time RT-PCR. *Nucleic Acids Res* **29**, e45.

**Sakamoto, T., Murata, N. & Ohmori, M. (1991).** The concentration of cyclic AMP and adenylate cyclase activity in cyanobacteria. *Plant Cell Physiol* **32**, 581-584.

**Sato, S., Shimoda, Y., Muraki, A., Kohara, M., Nakamura, Y. & Tabata, S. (2007).** A large-scale protein protein interaction analysis in *Synechocystis* sp. PCC 6803. *DNA Res* **14**, 207-216.

**Singh, A. K., Elvitigala, T., Bhattacharyya-Pakrasi, M., Aurora, R., Ghosh, B. & Pakrasi, H. B. (2008).** Integration of carbon and nitrogen metabolism with energy production is crucial to light acclimation in the cyanobacterium *Synechocystis*. *Plant Physiol.* **148**, 467-78

**Stanier, R. Y., Kunisawa, R., Mandel, M. & Cohen-Bazire, G. (1971).** Purification and properties of unicellular blue-green algae (order Chroococcales). *Bacteriol Rev* **35**, 171-205.

**Stevens, D. R., Rochaix, J. D. & Purton, S. (1996).** The bacterial phleomycin resistance gene *ble* as a dominant selectable marker in *Chlamydomonas*. *Mol Gen Genet* **251**, 23-30.

**Su, Z., Oلمان, V., Mao, F. & Xu, Y. (2005).** Comparative genomics analysis of NtcA regulons in cyanobacteria: regulation of nitrogen assimilation and its coupling to photosynthesis. *Nucleic Acids Res* **33**, 5156-5171.

**Subramaniam, S. (1998).** The Biology Workbench--a seamless database and analysis environment for the biologist. *Proteins* **32**, 1-2.

- Sugishima, M., Hagiwara, Y., Zhang, X., Yoshida, T., Migita, C. T. & Fukuyama, K. (2005).** Crystal structure of dimeric heme oxygenase-2 from *Synechocystis* sp. PCC 6803 in complex with heme. *Biochemistry* **44**, 4257-4266.
- Summerfield, T. C. & Sherman, L. A. (2008).** Global transcriptional response of the alkalitolerant cyanobacterium *Synechocystis* sp. strain PCC 6803 to pH 10. *Appl Environ Microbiol.* **74**, 5276-5284
- Summers, M. L., Wallis, J. G., Campbell, E. L. & Meeks, J. C. (1995).** Genetic evidence of a major role for glucose-6-phosphate dehydrogenase in nitrogen fixation and dark growth of the cyanobacterium *Nostoc* sp. strain ATCC 29133. *J Bacteriol* **177**, 6184-6194.
- Terauchi, K. & Ohmori, M. (1998).** An adenylate cyclase, CyaD, mediates the signal of blue light in the cyanobacterium *Synechocystis* sp. PCC 6803. *Plant Cell Physiol* **39**, 153.
- Terauchi, K. & Ohmori, M. (1999).** An adenylate cyclase, Cya1, regulates cell motility in the cyanobacterium *Synechocystis* sp. PCC 6803. *Plant Cell Physiol* **40**, 248-251.
- Terauchi, K. & Ohmori, M. (2004).** Blue light stimulates cyanobacterial motility via a cAMP signal transduction system. *Mol Microbiol* **52**, 303-309.
- Vogel, J., Axmann, I. M., Herzel, H. & Hess, W. R. (2003).** Experimental and computational analysis of transcriptional start sites in the cyanobacterium *Prochlorococcus* MED4. *Nucleic Acids Res* **31**, 2890-2899.
- Xu, M. & Su, Z. (2009).** Computational prediction of cAMP receptor protein (CRP) binding sites in cyanobacterial genomes. *BMC Genomics* **10**, 23.
- Yoshimura, H., Hisabori, T., Yanagisawa, S. & Ohmori, M. (2000).** Identification and characterization of a novel cAMP receptor protein in the cyanobacterium *Synechocystis* sp. PCC 6803. *J Biol Chem* **275**, 6241-6245.
- Yoshimura, H., Yanagisawa, S., Kanehisa, M. & Ohmori, M. (2002a).** Screening for the target gene of cyanobacterial cAMP receptor protein SYCRP1. *Mol Microbiol* **43**, 843-853.
- Yoshimura, H., Yoshihara, S., Okamoto, S., Ikeuchi, M. & Ohmori, M. (2002b).** A cAMP receptor protein, SYCRP1, is responsible for the cell motility of *Synechocystis* sp. PCC 6803. *Plant Cell Physiol* **43**, 460-463.
- Zhang, X., Migita, C. T., Sato, M., Sasahara, M. & Yoshida, T. (2005).** Protein expressed by the *ho2* gene of the cyanobacterium *Synechocystis* sp. PCC 6803 is a true heme oxygenase. Properties of the heme and enzyme complex. *FEBS J* **272**, 1012-1022.

1 **Fig. 1.** Electromobility gel shift assay demonstrating bound His-Sycrp1/DNA complexes  
2 and unbound DNA. The indicated 40 bp radiolabeled dsDNA oligonucleotides  
3 surrounding previously proposed Crp binding sequences (Table 1) are indicated. (a)  
4 Side-by-side comparison of all targets predicted by Ochoa de Alda & Houmard (2000).  
5 Labeled *slr1667* and Rndm. oligonucleotides are included as positive and negative  
6 controls, respectively. (b) Competitive binding to high affinity, and (c) low affinity Crp  
7 binding sequences. Unlabeled competitor was added as indicated in addition to reaction  
8 buffers containing: (a) and (c) 500.0 nM His-Sycrp1, 20.0  $\mu$ M cAMP, 500.0 nM  
9 unlabeled double stranded Rndm. Oligonucleotide, and 1.0 nM of the labeled dsDNA  
10 indicated; (b) 100 nM His-Sycrp1, 20.0  $\mu$ M cAMP, and 1.0 nM of the labeled dsDNA  
11 indicated. Running buffers and 10 % acrylamide composition was: (a) and (c)  $0.25 \times$   
12 TBE pH 8.0 at 4  $^{\circ}$ C, 20  $\mu$ M cAMP, and 50:1 (w/w) acrylamide to bis-acrylamide ratio,  
13 (b)  $1.0 \times$  TAE pH 8.0 at 4  $^{\circ}$ C, 20  $\mu$ M cAMP, and 30:0.8 (w/w) acrylamide to bis-  
14 acrylamide ratio.  
15

16 **Fig. 2.** Relative gene expression during environmentally induced low to high [cAMP] in  
17 both Wt and *crp* mutant strains of *Synechocystis* and *E. coli* for indicated genes. (a), (b),  
18 and (c) *Synechocystis* cells were acclimated to the dark for 16 h. (low [cAMP]) and  
19 transferred to the light (high [cAMP]). Cells were collected for RNA quantification by  
20 RT-QPCR in the dark (black bars), 30 min (grey bars), and 60 min (white bars) following  
21 illumination. (d), (e), and (f) *E. coli* M182 cells containing the intergenic region of the  
22 indicated *Synechocystis* gene oriented to drive transcription of a promoterless *gfp* reporter  
23 were grown in either LB containing 3% glucose (low [cAMP], black bars) or LB alone  
24 (high [cAMP], white bars). The black bars in (a), (b), (d), and (e) are calibrators  
25 presented for ease of reference only and do not contain error as defined (Pfaffl, 2001).  
26 The Y-axis label in (a), (b), and (c) is defined by Pfaffl (2001): “Expression Ratio of a  
27 *sample* versus a *control* in comparison to a reference gene” =  $(E_{\text{target}})^{\Delta CP_{\text{target}}}$   
28  $((E_{\text{reference}})^{\Delta CP_{\text{reference}}})^{-1}$  where  $\Delta CP$  is the QPCR cycle threshold of the *control* – *sample*,  
29 target is the gene of interest, reference is *mpB*, and  $E$  is PCR amplification efficiency.  
30 When Wt expression is the *sample* and, Wt expression during the low [cAMP] condition  
31 (Wt low [cAMP]) is the *control*, the experimentally modified independent variable is  
32 time of illumination that causes high [cAMP]. The same holds for *crp* vs. *crp* low  
33 [cAMP]. When Wt is the *sample*, and *crp* is the *control*, the experimentally modified  
34 independent variable is Crp. All samples were cultured in triplicate (n = 3), and error  
35 bars indicate  $\pm$  SE. Note the log scale in top graphs and value break in (f).  
36

37 **Fig. 3.** Promoter regions of *crp* target genes in *Synechocystis*. (a) Upstream regions of  
38 *murF* homologues in closely related cyanobacteria. CwatDRAFT\_4119 and  
39 CY0110\_02369 correspond to those indicated ORF identifiers in *Crocospaera watsonii*  
40 and *Cyanotheca* sp. CCY 0110 respectively. MSA’s span conserved Crp sites to the  
41 conserved N-terminal amino acids belonging to protein homologues, thereby anchoring  
42 the alignment between two conserved regions. (b) Partial upstream region of *chlAII*. (c)  
43 Upstream regions of *slr1268* and *slr0442*. A secondary low affinity site proposed by  
44 Omagari *et al.* (2008) is boxed with dashes. Proposed Crp binding sites identified by  
45 competitive gel shift in Fig. 1 are boxed. All putative transcriptional start sites were  
46 determined by RACE mapping in this work, are labeled (*gene P<sub>x</sub>*), and enclosed with

47 small boxes. Suggested -10 sigma factor binding sites are underlined. Annotated  
 48 translational start codons are double underlined. Tic marks are spaced 10.5 bases apart  
 49 for reference. The *murF* P<sub>1</sub> is not shown, but described in the text.

**Table 1:** One strand (complement not shown) of double-stranded blunt-end Oligonucleotide DNA used in EMSA and the calculated  $\Delta\Delta G^A_{total}$  free energy change from consensus. The putative Sycrp1 core binding consensus is indicated in bold.

Gene	Sequence	$\Delta\Delta G^A_{total}$
<b><u>slr1667</u></b> Target of Sycrp1	ATACACAACAGTTGTGATCTGGGTCACAACCATTTGAGTGA	# ‡ <b>0.34</b>
Rndm. (neg. control)	AAGCCGTAAGACCTAATGTAGAAGTGCTCCAGAAGCTCAC	19.89
slr1991 <i>cydA</i>	AGGCTCCCTGATGGGGACAGCGGTCACGGACCTTTACTTT	* 5.85
sll0065 <i>ilvN</i>	TTCCCTAACTCTAGTGAGGAATTTTGCAAAAATGCAAGCTT	* 8.04
slr0194 <i>rpiA</i>	AACCGGAACCTGTTCTGATAATGTTTCGCACTGTAGAGATTT	* 9.01
<b><u>slr1351 murF</u></b> /sll1247 hyp.	GCACCCATGGGAGGTGATCTAGATCACAGATAAAAAATTGC	#*†‡ <b>0.67</b>
slr1575 hyp.	GCGGAGACAAAATGGGAAATCACTCACGCCTCGTCTCAAT	* 7.35
sll1708 <i>narL</i> /slr1805 <i>hik16</i>	CGGCACCCTTACCGTGATAGTAATCACCGATGAAGTACAA	#*†‡ <b>3.07</b>
sll0682 <i>pstA</i>	GGCAGAACTGATTGTGAACAAAAGTCAAAGCTAAATATTAG	* 7.85
sll0041 <i>cheD</i>	GACATTACCTGGTGTGAAACGGATCAAATTCATCTCCCC	* 6.84
slr1200 <i>livH</i>	CAATGGCAACAATGTGATAATCCCCACACCTGCCCCACG	* 4.12
<b><u>sll1874 at103, chlA<sub>II</sub></u></b>	CCTTCCACTGCTTGTGAGAAATAATCACAGGCAGTTTTTTT	#*†‡ <b>2.62</b>
slr1279 <i>ndhC</i>	CGGGCACCGAAATGTGAATCGTTTCAGAATTGGATTATTG	* 3.49
<b><u>slr0442 hyp.</u></b> /sll1520 <i>recN</i>	TGGTTGGAGGGCTGTGATCCAGATCACATACGTGGGTAA	# †‡ <b>0.00</b>
sll1268 hyp.	TCACCCAATAGTTGTGATCTAGATCACAGAGGGCCACGGC	# †‡ <b>0.00</b>

# Sycrp1 binding sequences proposed by Xu & Su (2009).

\* Sycrp1 binding sequences proposed by Ochoa de Alda & Houmard (2000).

† Sycrp1 binding sequences proposed by Omagari *et al.* (2008) demonstrate His-Sycrp1 binding.

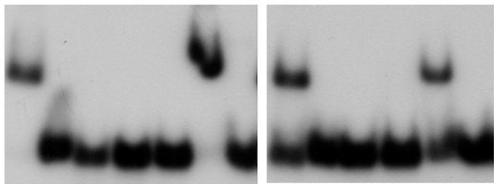
‡ Oligonucleotide sequences demonstrating sequence-specific His-Sycrp1 binding in this work.

ORF identifiers of genes demonstrating both sequence-specific binding and *sycrp1*-dependent transcriptional regulation are bold underlined. In bold are  $\Delta\Delta G^A_{total}$  values < 3.1. The value of  $\Delta\Delta G^A_{total}$  was calculated by strict summation of position values given by the position specific scoring matrix in Omagari *et al.*, (2008) except that G and C substitution  $\Delta G$  values at positions 9 and 14 were switched to accurately reflect the authors' intent.

50

51

(a)



slr1667  
Rndm.  
slr1991  
sl10065  
slr0194  
slr1351/sll1247  
slr1575  
sll1708/slr1805  
sll0682  
sll0041  
slr1200  
sll1874  
slr1279

(b)

Unlabeled  
Competitor  
Added

none  
10.0 nM slr1667  
100.0 nM slr1667  
100.0 nM Rndm.

Slr1351  
/sll1247

slr0442  
/sll1520

sll1268



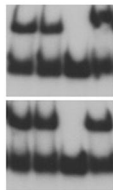
(c)

Unlabeled  
Competitor  
Added

none  
10.0 nM slr1667  
100.0 nM slr1667  
100.0 nM Rndm.

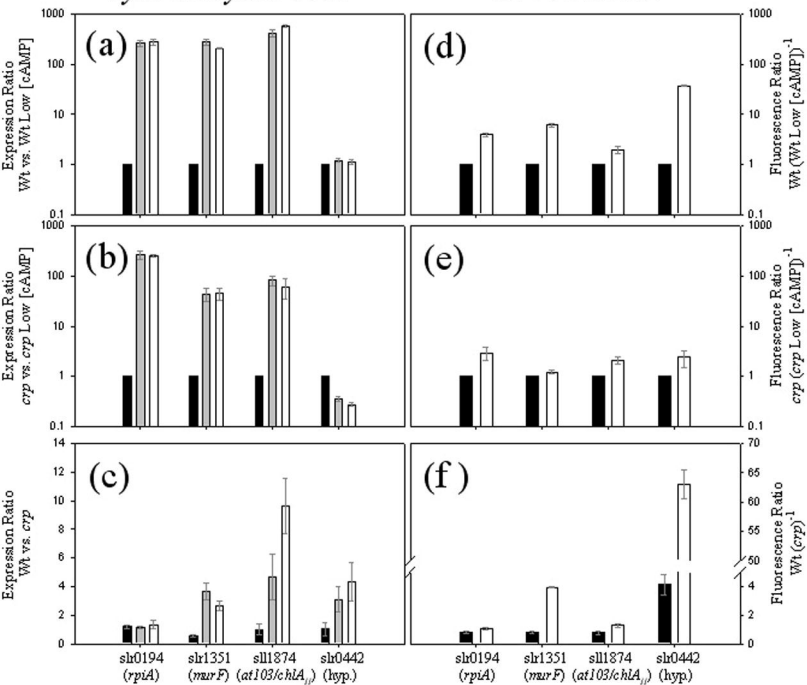
Sll1874

sll1708  
/slr1805



*Synechocystis* 6803

*E. coli* M182



(a)

```

CwatDRAFT 4119 nrIF |TTTGTGTATGTGATCTTGATCACTAAAAATCGATTTTCTTGTATTTCAGTAATTTT-----CTATATTTTTCTCAGTAGTCATC
CY0110 U2369 nrIF |TTTTGTATGTGATCTTGATCACCACATTTCAATTAATTTTCTCGGTAATTTT-----CTCGTTTTATCTCAGTAGTTATT
slr1351 nrIF |CATGGGAGGTGATCTAGATCACAGATAAAAAATGCAAAATGACTTAACATTCCTGAGTCAATTCTAACTCAGTTTTCTCCGCCATATT
                                     nrIF P2

CwatDRAFT 4119 nrIF |CTAA-TAAGCAATATGATTCTAAGTGAAATCCCAATAT-----TTTG---TCCAAAAATTTA-AAATCTGTGTA-----A
CY0110 U2369 nrIF |CCAGGTTGTTACTATGATTCTCCGTGAAATTCACACTAT-----CCTG---TCCGGCACTTTC-CAAAGATATCAC-----A
slr1351 nrIF |T-----TCACTCCTATTCTTTCCCATGAACTCCAAACTTTCCCTATTTGACA TCCGTACATTCTAGAAAGTGTGTATTGTCTGTTACCA
                                     nrIF P3

CwatDRAFT 4119 nrIF |AATTTGATGGT
CY0110 U2369 nrIF |AATTTGATGGA
slr1351 nrIF |GTTTTGATGGC

```

(b)

```

slr1874 chlAII |CCTTCCACTGC|TGTGAGAATAATCACAGGCAGTTTTTTT- N242 - TCTTGTCCAGGATCCGGGGAATTGGACAGGATGAAAAGCCACAT
                                     slr1874 P1

```

(c)

```

slr1268 |TTTTCAGGCTATAGAAAGTGGTCTGGGTCAACC AATAGTTGTGATCTAGATCACAGAGGGCCACGGCCCTGGATCTCTACAAATGGTCAAT--
slr0442 |GTAGGTTAGGCTTAGGGTTAATGATGTTGGTGGAGGGCTGTGATCCAGATCACATACGTTGGGTTAACCGGGATAATAAATAACAGTTTGG
                                     slr0442 P1
                                     slr0442 P2

slr1268 P1
slr1268 |-----GGCAGTATGCCTAATCTGCCTGTTTGGGGCCATGCAAAGGACATAGTTTTCTATGGTTAGTCCAGGTTTGACGCCTCTGCCAA
slr0442 |TGAAATGAAGGGTGGTGGTAGAGAGTTGACCCAGCTTCAAACAAGAACC AAAGTTCAGTGTTCCTAATGTAAT-----CGTTTGTTTTTA

slr1268 |AGTCCCTCCACCTGCCTGGTTGCTT-TTAAATGAAACTGACCTTTGTAGGGATCGAAGGGTAATTATGAA
slr0442 |TTTTCTTTATTGATGCTTTCTATCTCGCTCACTTTATTTTTACTCACAGTTGAAGATCAATTAAGAA

```